**Annales
Geophysicae**

Error analysis of Abel retrieved electron density profiles from radio occultation measurements

X. Yue[1,3], **W. S. Schreiner**[1], **J. Lei**[2], **S. V. Sokolovskiy**[1], **C. Rocken**[1], **D. C. Hunt**[1], and **Y.-H. Kuo**[1]

[1]COSMIC Program Office, University Corporation for Atmospheric Research, Boulder, CO, USA
[2]Department of Aerospace Engineering Sciences, University of Colorado, Boulder, CO, USA
[3]Institute of Geology and Geophysics, Chinese Academy of Sciences, Beijing, China

Abstract. This letter reports for the first time the simulated error distribution of radio occultation (RO) electron density profiles (EDPs) from the Abel inversion in a systematic way. Occultation events observed by the COSMIC satellites are simulated during the spring equinox of 2008 by calculating the integrated total electron content (TEC) along the COSMIC occultation paths with the "true" electron density from an empirical model. The retrieval errors are computed by comparing the retrieved EDPs with the "true" EDPs. The results show that the retrieved NmF2 and hmF2 are generally in good agreement with the true values, but the reliability of the retrieved electron density degrades in low latitude regions and at low altitudes. Specifically, the Abel retrieval method overestimates electron density to the north and south of the crests of the equatorial ionization anomaly (EIA), and introduces artificial plasma caves underneath the EIA crests. At lower altitudes (E- and F1-regions), it results in three pseudo peaks in daytime electron densities along the magnetic latitude and a pseudo trough in nighttime equatorial electron densities.

Keywords. Ionosphere (Equatorial ionosphere; Instruments and techniques) – Radio science (Space and satellite communication)

1 Introduction

Since the success of the Global Positioning System/Meteorology (GPS/MET) experiment aboard the MicroLab 1 satellite, low Earth orbit (LEO) based radio occultation (RO) has become an important technique for sounding the Earth's atmosphere. It provides vertical profiles of refractivity, neutral density, temperature, pressure, and water vapor in the stratosphere and troposphere and electron density in the ionosphere (Hajj and Romans, 1998; Rocken et al., 2000; Schreiner et al., 1999). These parameters are useful for both numerical weather forecasting and scientific research (Rocken et al., 2000). The electron density profile (EDP) is one of the most important products for space weather and ionospheric science. In order to retrieve EDP from the integrated slant total electron content (TEC), many different methods have been applied (e.g., Hernández-Pajares et al., 2000; Schreiner et al., 1999; Tsai and Tsai, 2004; Wu et al., 2009b), but Abel inversion is the most commonly used technique.

To date, the Constellation Observing System for Meteorology Ionosphere and Climate /Formosa Satellite 3 (COSMIC/FORMOSAT-3), a joint US/Taiwan radio occultation mission consisting of six identical micro-satellites, has produced over 2.1 million EDPs. At the COSMIC Data Analysis and Archive Center (CDAAC) of the University Corporation for Atmospheric Research (UCAR), EDPs are retrieved by the Abel inversion from TEC along the LEO-GPS ray. Detailed descriptions of CDAAC data processing and the EDP retrieval method can be found in Kuo et al. (2004), Lei et al. (2007), Schreiner et al. (1999), and Syndergaard et al. (2006). These EDPs have been validated by comparing with ground-based Ionosonde and Incoherent Scatter Radar (ISR) observations (e.g., Lei et al., 2007; Kelley et al., 2009). However, it is difficult to quantitatively evaluate the Abel retrieval error globally because there are not enough coincidences between RO and independent observations to provide good temporal and spatial coverage.

The RO EDP retrieval approach relies on a few assumptions and approximations and the spherical symmetry assumption used in Abel inversion is thought to be the most significant error source (Lei et al., 2007; Schreiner et al., 1999; Wu et al., 2009a). Wu et al. (2009b) found a good correlation between the retrieval error and the asymmetry factor by a simulation study. Straus (2007) showed that Abel
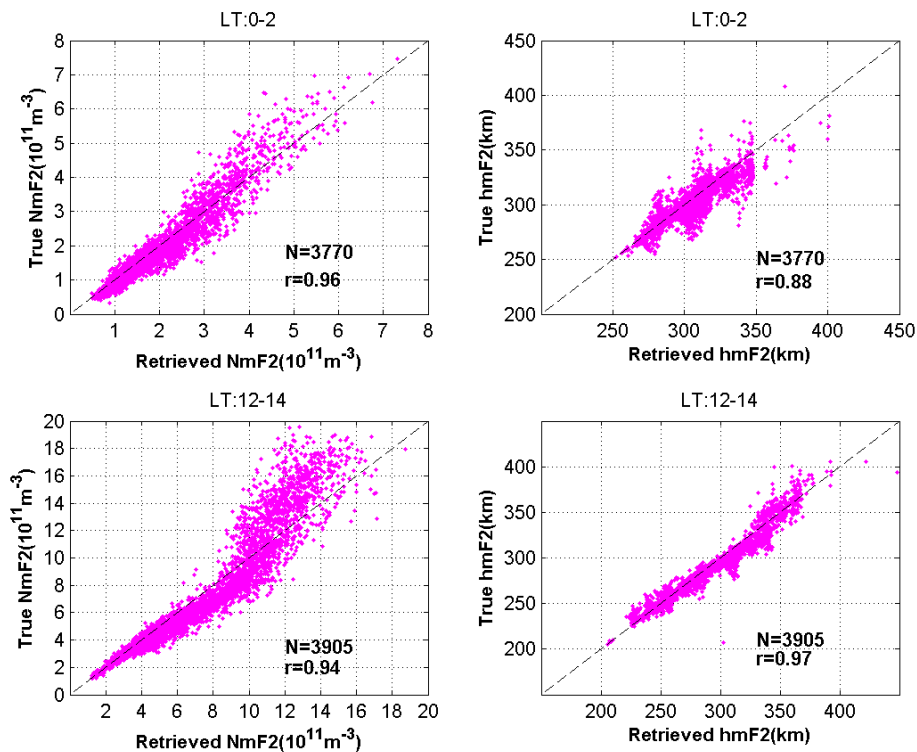
AnGeo Communicates

Fig. 1. Correlation between the true and retrieved *Nm*F2 (left panels) and *hm*F2 (right panels) during nighttime (00:00–02:00 LT, upper panels) and daytime (12:00–14:00 LT, bottom panels). The sample numbers and correlation coefficients are given in the panels.

retrieved *Nm*F2 and *hm*F2 have relatively significant errors at low altitude. Wu et al. (2009a) obtained generally the similar results as Straus (2007) by a simulation work and comparison between COSMIC observations and ionosondes. However, both studies of Straus (2007) and Wu et al. (2009a) did not address the errors of Abel retrieved EDPs below the F2 layer. This study will carry out a simulation study of the Abel-inversion induced EDP errors caused by the horizontal inhomogeneity of electron density in a systematic way, and will quantitatively provide the errors distributions versus altitude (from E-layer to the topside ionosphere) for the first time.

2   Methodology

This research performs a simulation study based on the geometry of the observed COSMIC occultation events. For each occultation event, slant TECs observed by the COSMIC along the LEO-GPS ray are replaced with those from an empirical model (i.e. "truth"). This simulated TEC calculation consists of integration of the electron density along the straight-line between the LEO receiver and GPS transmitter. Note that effects of ray bending are ignored and measurement noise is not considered in this study. An integration resolution of 50 km was used to produce TEC with sufficient convergence. The simulated TEC is then inverted into an

EDP along the tangent points by the same Abel inversion software that is used for CDAAC EDP retrieval. Finally, the error of the retrieval method is calculated by comparing the retrieved EDP with the EDP from the empirical model at the ray tangent points. Hereafter, the modeled and the occultation-retrieved electron density are referred to as true and retrieved electron density, respectively.

The empirical ionosphere electron density model used here is NeQuick, which is developed by the International Center for Theoretical Physics in Italy and the University of Graz in Austria. It represents the EDP by Epstein functions based on the CCIR model of ionospheric characteristics up to an altitude of several thousands km (Leitinger et al., 2002). The version we used here is NeQuick-ITUR, which is the recommended version by the ITU-R for the public. NeQuick has comparable accuracy with IRI model in both E- and F-layers and can give reasonable EDPs. The period during the day of year (DOY) 70–100, 2008 is selected in this simulation (about one month centered at spring equinox). The observed F10.7 radio flux downloaded from the ftp site of National Geophysical Data Center (NGDC) was used as input to the NeQuick model. 43 180 COSMIC occultation events were simulated during the studied period.

3 Results

Figure 1 shows comparisons between true and retrieved *Nm*F2 (left panels) and *hm*F2 (right panels) for nighttime 00:00–02:00 LT (upper panels) and daytime 12:00–14:00 LT (bottom panels). The sample numbers and the correlation coefficients are also given in the panels. Generally, the retrieved *Nm*F2 and *hm*F2 are in good agreement with the true values, except for large daytime *Nm*F2. The absolute (and relative) standard deviations of the differences between the retrieved and true values are 3.2×10^{10} m^{-3} (16%) and 1.4×10^{11} m^{-3} (15%) for nighttime and daytime *Nm*F2, and 8.9 km (2%), 7.4 km (2%) for nighttime and daytime *hm*F2, respectively.

Figure 2 shows the daytime true electron density (a), retrieved electron density (b), absolute deviation (c), and relative deviation (d) between the retrieved and the true electron density as a function of magnetic latitude and altitude (the simulated data have been collected between 12:00–14:00 LT over the one month period). Figure 2a and b shows the well-known EIA, which is almost symmetrically distributed with respect to the geomagnetic equator around equinox. Generally, the retrieved EDPs reasonably represent the EIA and track the latitudinal and height variations of the true electron density modeled by NeQuick. Figure 2c and d gives quantitative representations of the difference between the true and retrieved electron densities. The most prominent feature is that the retrieved electron density underestimates the true electron density in the region surrounding the EIA crest ($\pm 10°$–30° latitude), while overestimates near the equator ($\pm 10°$) and in the north and south of the EIA crests ($\pm 30°$–50°). The bias for large electron density in the daytime *Nm*F2 comparison (Fig. 1) also indicates the underestimation of the retrieved density at the daytime EIA crests. Two plasma depletions are seen clearly underneath the EIA peaks in the retrieved electron density, but not in the true electron density. Three obvious peaks and two troughs are present in the absolute retrieval error along latitude. Note that the retrieval errors are relatively small in the topside ionosphere at low latitudes and at all altitudes in middle and high latitudes.

Both the relative and absolute errors have similar latitudinal variations but the relative retrieval errors decrease more rapidly with altitude due to small electron density at low altitudes. The retrieval method overestimates the true electron density by more than 200% near the E-layer at latitudes $\pm 30°$–50°. In the equatorial region ($\pm 10°$), the errors can be up to 100%. Underneath the EIA crests, the underestimations reach -200% and result in negative electron densities in the E-region.

Figure 3 demonstrates distributions of electron density and errors at 110 km (left panels) and 220 km altitude (right panels) as a function of geographic latitude and longitude during 10:00–12:00 UT. The true and retrieved electron densities are given in the upper two panels. The true electron density at 110 km has a peak over the equator, as the result of solar irradiation. At 220 km, there are two peaks featured
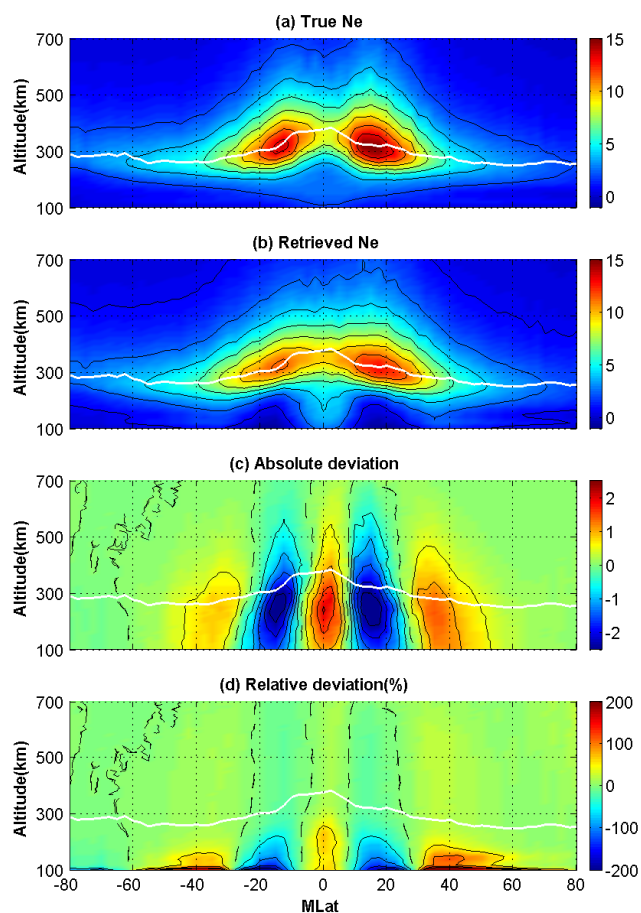

Fig. 2. Geomagnetic latitudinal and altitudinal variations of true electron density (**a**), retrieved electron density (**b**), absolute deviation (**c**) and relative deviation (**d**) between retrieved and true electron density during 12:00–14:00 LT. The white lines indicate the *hm*F2 of true electron density. The unit in panels (a–c) is 10^{11} m^{-3} and in panel (d) is percentage. The dashed lines in panels (c) and (d) indicate zero values. The intervals between the contour lines in (c) and (d) are 0.5×10^{11} m^{-3} and 50%, respectively.

at different latitudes, because of the equatorial fountain effect. The retrieved electron densities differ significantly from the truth. For both selected altitudes, the absolute deviation shows three peaks and two troughs along the latitude direction during the daytime, which is consistent with the results in Fig. 2. The EIA evolves from two peaks in the low latitude during daytime to a single peak over the equatorial region at night. The locations of the underestimation surrounding the EIA crests also shift from the low latitude to the equatorial region.

The relative deviations in Fig. 3d indicate that the retrieval errors during daytime mainly occur in middle and low latitudes. During nighttime, besides the underestimation over the equatorial region, the overestimation appears in most regions, especially at 110 km. At 110 km, there are three peaks in the retrieved electron density along the latitude during
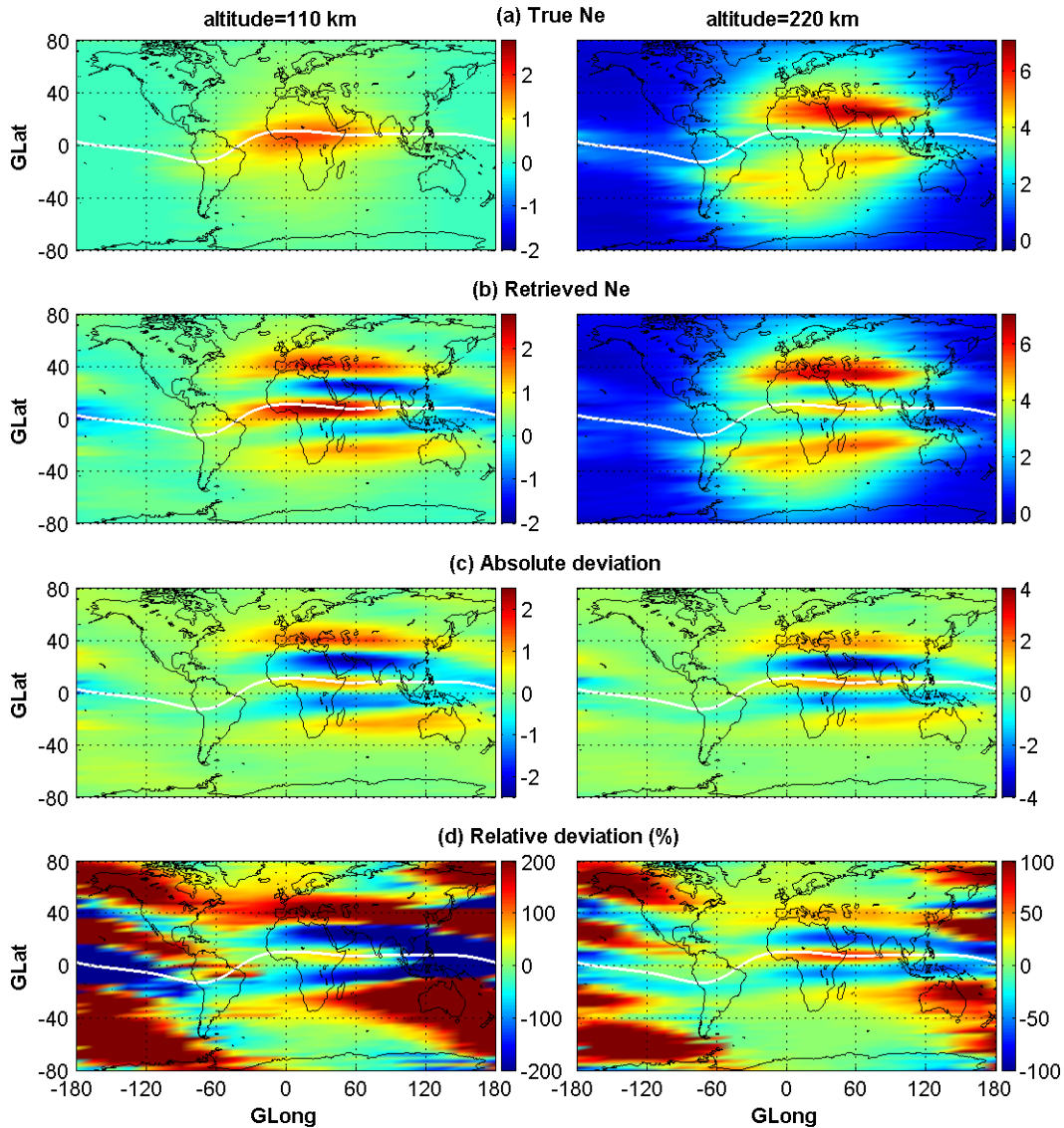
Fig. 3. Geographic longitudinal and latitudinal variations of true electron density **(a)**, retrieved electron density **(b)**, absolute deviations **(c)** and relative deviations **(d)** between retrieved and true electron density during 10:00–12:00 UT. Left and right panels are for 110 and 220 km altitudes. The white lines indicate the DIP equator. The unit in panels (a–c) is 10^{11} m^{-3} and in panels (d) is percentage.

daytime, although only a single peak exits in the true electron density; at nighttime, a trough can be seen clearly over the equatorial region in the retrieved electron density, whereas it is not present in the true electron density. A similar situation also occurs in the retrieved electron density at 220 km, except that there are two peaks in true electron density along the latitude during daytime.

4   Discussion

The retrieved NmF2 and hmF2 in Fig. 1, in general, show good correlation with the true values. The standard deviation of the relative retrieval error is ∼15% for NmF2 and ∼2%

for hmF2. This demonstrates that the retrieved NmF2 and hmF2 are reliable. Our simulations are consistent with previous validation results comparing real retrievals to ionosondes by several authors (Hajj and Romans, 1998; Lei et al., 2007; Wu et al., 2009a), although actual retrieval errors from observations may be different with those from the simulation where a relative smooth model is used. Hajj and Romans (1998) compared the GPS/MET observed NmF2 with collocated ionosonde observations and their results showed agreement of about 20%. The comparison of NmF2 between COSMIC and 31 globally distributed ionosondes by Lei et al. (2007) showed a correlation coefficient of ∼0.85. On the other hand, our simulations showed the retrieval daytime

*Nm*F2 is lower than the true values in the EIA crests, while slightly larger than the true values over the equator. Lei et al. (2007) compared COSMIC EDPs with ISR observations at Millstone Hill (middle latitude) and Jicamarca (magnetic equator) and found that the agreement is better at Millstone Hill than Jicamarca, which is also consistent with our simulation results.

Our simulations demonstrate that the Abel retrieval method introduces significant errors in electron densities in the low latitude region. It overestimates electron density in the north and south of the EIA crest region, but underestimates the electron density surrounding the EIA crests. We checked the COSMIC observed EDPs during the simulated period and found obvious plasma caves underneath the EIA crests and three peak feature during daytime and a trough at night in the E layer along the latitude (figures not shown). The simulation work was also applied for the summer solstice and our obtained conclusion about Abel retrieval error is not altered, except a little difference in the locations of underestimation and overestimation because the EIA distributes asymmetrically with respect to equator during summer solstice. These retrieved errors potentially may affect results of the studies based on Abel-retrieved EDPs, such as the E-layer three peaks found by Chu et al. (2009), the empirical modeling results for *fo*F1 and *fo*E by Tsai et al. (2009).

The results in Figs. 2–3 also revealed that the current retrieval method has relatively poor performance at lower altitudes. The same conclusion was drawn from the comparison between COSMIC EDPs with Arecibo ISR observations (Kelley et al., 2009). Thus data users should be aware of this limitation of the Abel retrieved electron density from the radio occultation measurements when they use the Abel retrieved EDPs to conduct scientific research on the ionospheric phenomena at low altitudes, such as E-layer, sporadic E-layer and the F1 layer.

The error distributions simulated in this study are explained by the spherical symmetry assumption. The spherical symmetry assumption is not satisfied at low latitudes where electron density has strong horizontal gradients. When the tangent points are in the EIA crest regions, electron densities are underestimated because the real slant TEC does not support high values in that spherical layer. In the nearby region the electron density will be overestimated because the effects of EIA peak region are spread by the inversion under the spherical symmetry assumption. Solomon et al. (1984) also found that the true values underneath the peak usually are underestimated when they retrieved the volume emission rate of thermospheric airglow from satellite photometry in a limb-viewing geometry. At low altitudes, the relative errors are larger than in the F-region because of the downward error propagation from F2 layer where horizontal gradients of electron density are large and lower background electron density at low altitudes (Schreiner et al., 1999).

Horizontal electron density gradients in the zonal direction also can result in errors in the Abel retrieval process. For ex-

ample, the ray between GPS and LEO may go through different local time zones across the terminator. There are also two pseudo plasma caves underneath the EIA crests when the occultation events with zonal LEO-GPS rays are used in the retrieval, but the resultant plasma caves are weaker than the pseudo caves retrieved from the occultation observations along the rays going through the meridional direction (figure not shown). This is due to that horizontal extensions of EIA are larger in the zonal direction than in the meridional one.

5 Conclusion

In this paper, through a simulation study we investigated the error distribution of the Abel inversion, which is often used to derive EDPs from RO data. We simulated the occultation events observed by the COSMIC satellites during the spring equinox of 2008 and calculated the integrated TEC along the COSMIC occultation paths by using the NeQuick EDPs ("true" EDPs). The retrieval errors are estimated by comparing the EDPs retrieved from modeled TEC with the true EDPs. Generally, the retrieved *Nm*F2 and *hm*F2 are in good agreement with the true values, whereas the current Abel retrieval method introduces significant errors in electron densities in low latitude regions and at low altitudes. It overestimates the electron density in the north and south of the EIA crests, but underestimates the electron density surrounding the EIA crests. At lower altitudes (E- and F1-regions), the retrieval errors result in three pseudo peaks in daytime electron densities along magnetic latitude and a pseudo trough in nighttime equatorial electron densities.

Our simulation provides a guide to users of the Abel retrieved EDPs, especially at low latitude regions and low altitudes. This study also provides an important insight to improve the Abel inversion retrieval method in the future. Improvements are currently under investigation at the CDAAC. Some new and improved retrieval methods, such as adding other observations or nearby occultation observations or modeling results to provide horizontal gradient (Hernández-Pajares et al., 2000; Schreiner et al., 1999; Tsai and Tsai, 2004), correcting the retrieved EDPs by making use of the relationship between retrieval error and electron density asymmetry (Wu et al., 2009b), or data assimilation method (Nicolls et al., 2009), will be applied and compared in a future study.

References

Chu, Y. H., Wu, K.-H., and Su, C.-L.: A new aspect of ionospheric E region electron density morphology, J. Geophys. Res., 114, A12314, doi:10.1029/2008JA014022, 2009.

Hajj, G. A. and Romans, L. J.: Ionospheric electron density profiles obtained with the Global Positioning System: Results from the GPS/MET experiment, Radio Sci., 33(1), 175–190, 1998.

Hernández-Pajares, M., Juan, J. M., and Sanz, J.: Improving the Abel inversion by adding ground GPS data to LEO radio occultations in ionospheric sounding, Geophys. Res. Lett., 27, 2473–2476, 2000.

Kuo, Y.-H., Wee, T.-K., Sokolovskiy, S., Rocken, C., Schreiner, W., Hunt, D., and Anthes, R. A.: Inversion and error estimation of GPS radio occultation data, J. Meteorol. Soc. Jpn., 82(1B), 507–531, 2004.

Kelley, M. C., Wong, V. K., Aponte, N., Coker, C., Mannucci, A. J., and Komjathy, A.: Comparison of COSMIC occultation-based electron density profiles and TIP observations with Arecibo incoherent scatter radar data, Radio Sci., 44, RS4011, doi:10.1029/2008RS004087, 2009.

Lei, J., Syndergaard, S., Burns, A. G., et al.: Comparison of COSMIC ionospheric measurements with ground-based observations and model predictions: Preliminary results, J. Geophys. Res., 112, A07308, doi:10.1029/2006JA012240, 2007.

Leitinger, R., Radicella, S., and Nava, B.: Electron density models for assessment studies – new developments, Acta Geodet. Geophys. Hung, 37, 183–193, 2002.

Nicolls, M. J., Rodrigues, F. S., Bust, G. S., and Chau, J. L.: Estimating E region density profiles from radio occultation measurements assisted by IDA4D, J. Geophys. Res., 114, A10316, doi:10.1029/2009JA014399, 2009.

Rocken, C., Kuo, Y.-H., Schreiner, W., Hunt, D., Sokolovskiy, S., and McCormick, C.: COSMIC system description, Terr. Atmos. Oceanic Sci., 11(1), 21–52, 2000.

Schreiner, W. S., Sokolovskiy, S. V., Rocken, C., and Hunt, D. C.: Analysis and validation of GPS/MET radio occultation data in the ionosphere, Radio Sci., 34(4), 949–966, 1999.

Solomon, S. C., Hays, P. B., and Abreu, V. J.: Tomographic Inversion of Satellite Photometry, Appl. Optics, 23, 3409–3414, 1984.

Straus, P. R.: Ionospheric climatology derived from GPS occultation observations made by the ionospheric occultation experiment, Adv. Space Res., 39, 793–802, 2007.

Syndergaard, S., Schreiner, W. S., Rocken, C., Hunt, D. C., and Dymond, K. F.: Preparing for COSMIC: Inversion and analysis of ionospheric data products, in: Atmosphere and Climate: Studies by Occultation Methods, edited by: Foelsche, U., Kirchengast, G., and Steiner, A. K., pp. 137–146, Springer, New York, 2006.

Tsai, L.-C. and Tsai, W.-H.: Improvement of GPS/MET ionospheric profiling and validation using Chung-Li ionosonde measurements and the IRI model, Terr. Atmos. Oceanic Sci., 15, 589–607, 2004.

Tsai, L.-C., Liu, C. H., Hsiao, T. Y., and Huang, J. Y.: A near real-time phenomenological model of ionospheric electron density based on GPS radio occultation data, Radio Sci., 44, RS5002, doi:10.1029/2009RS004154, 2009.

Wu, X., Hu, X., Gong, X., Zhang, X., and Wang, X.: Analysis of inversion errors of ionospheric radio occultations, GPS Solut., 13, 231–239, doi:10.1007/s10291-008-0116-x, 2009a.

Wu, X., Hu, X., Gong, X., Zhang, X., and Wang, X.: An asymmetry correction method for ionospheric radio occultation, J. Geophys. Res., 114, A03304, doi:10.1029/2008JA013025, 2009b.